

Polymeric ion-gels containing an amino acid ionic liquid for facilitated CO₂ transport media

Shohei Kasahara, Eiji Kamio, Ayumi Yoshizumi and Hideto Matsuyama

*Center for Membrane and Film Technology,
Department of Chemical Science and Engineering, Kobe University,
1-1 Rokkodai-cho, Nada-ku, Kobe, Hyogo 657-8501, Japan.
Fax: +81-78-803-6180; Tel.: +81-78-803-6180;
E-mail: matuyama@kobe-u.ac.jp*

SUPPLEMENTARY INFORMATION

Table of contents

(1) Materials and general procedures for AAILs synthesis	1
(2) Investigation into inhibition of radical polymerization in AAILs	2-6
(3) Finger-pressure compression tests of AAIL-gels	7
(4) General procedures for AAIL-gel film preparation	7
(5) General procedures for gas permeability testing	8-9
(6) Comparison of the performances of ionic liquid-based CO ₂ separation membranes	9-11
References	11-12

(1) Materials and general procedures for AAIL synthesis

Tetrabutylphosphonium hydroxide ([P₄₄₄₄][OH], 40 wt% in water) was purchased from Sigma-Aldrich Co. (St Louis, MO, USA). Glycine (99.8%), lysine (>99.0%), serine (>99.0%) and proline (>99.0%) were purchased from Tokyo Chemical Industry Co. (Tokyo, Japan). Methanol (99.8%) was purchased from Wako Pure Chemicals Industry Ltd. (Osaka, Japan). Acetonitrile (99.90%) was purchased from Sigma-Aldrich Co. All reagents were used as received.

The synthesis procedures for the amino acid based ionic liquid (AAIL) were as reported previously.¹ Tetrabutylphosphonium type AAILs (tetrabutylphosphonium glycine ([P₄₄₄₄][Gly]), tetrabutylphosphonium lysine ([P₄₄₄₄][Lys]), tetrabutylphosphonium serine [P₄₄₄₄][Ser], and tetrabutylphosphonium proline ([P₄₄₄₄][Pro])) were synthesized following a neutralization procedure. An aqueous solution of [P₄₄₄₄][OH] was added to a slight excess of an equimolar amino acid (AA) aqueous solution to prepare the [P₄₄₄₄][AA] salts, with water formed as a byproduct. The product was dried *in vacuo* for more than 8 h at 313 K. A mixture of acetonitrile/ethanol was then added to recrystallize and remove unreacted amino acid. The filtrate was evaporated to remove solvent. The reaction ratios were 95.5, 93.2, 99.9 and 99.9% for [P₄₄₄₄][Gly], [P₄₄₄₄][Lys], [P₄₄₄₄][Ser] and [P₄₄₄₄][Pro], respectively. The structures of the resulting [P₄₄₄₄][AA]s were confirmed by ¹H NMR spectroscopy (Bruker Advance 500, Bruker BioSpin) and FT-IR (ALPHA FT-IR Spectrometer, Bruker Optics) measurements. ¹H-NMR data and FT-IR data of [P₄₄₄₄][AA]s were consistent with those reported in the literature.¹

(2) Investigation into inhibition of radical polymerization in AAILs

Michael addition

Michael addition between a primary or a secondary amine and an acrylate is a well-known reaction.² Because the AAILs contain a high concentration of amino acid anions, we checked for Michael addition of the amine group to the vinyl group of an acrylate monomer. Because the *e*-value of methyl acrylate (MA) was the highest among the acrylate monomers investigated in this work, MA was chosen as a representative example. [P₄₄₄₄][Gly] was used as the typical AAIL. The experiment was carried out as follows. Equal amounts of MA and [P₄₄₄₄][Gly] were mixed and homogenized by vigorous mixing. The solution was poured into a test tube irradiated by 365 nm UV light for 24 hours. The occurrence of Michael addition was evaluated by comparing the ¹H NMR spectrum of the resulting solution with that of the original MA. The ¹H NMR spectrum are shown in Figure S1(a).

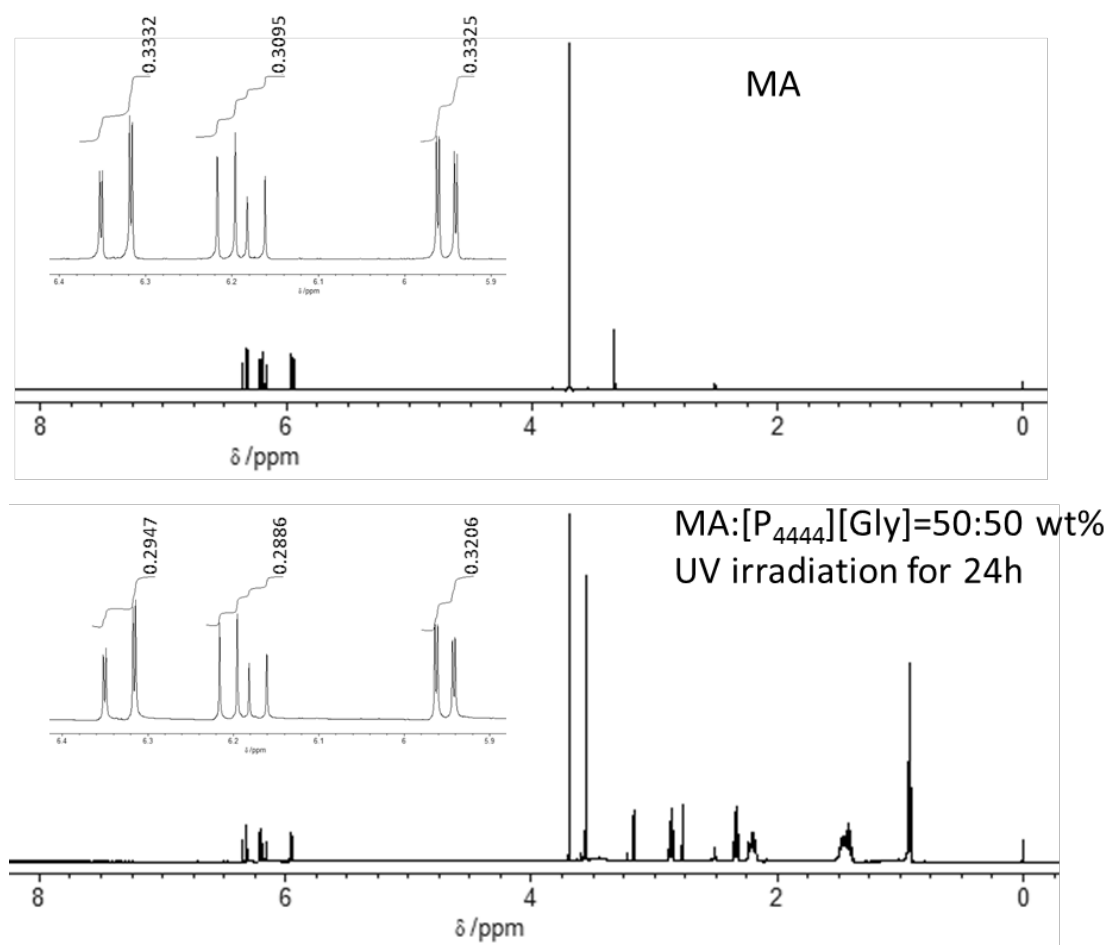


Figure S1(a) ¹H NMR spectra for MA and the MA/[P₄₄₄₄][Gly] mixture after UV irradiation for 24 h.

Comparing the two spectrum, the integration of the vinyl signal (δ 5.5–7.0 ppm, normalized by the integration of the methyl proton of MA) for the mixture of MA and $[P_{4444}][Gly]$ was not disappeared but decreased to 82% of that for MA. Because the molar ratio of $[P_{4444}][Gly]/MA$ in the 50:50 wt% MA/ $[P_{4444}][Gly]$ mixture is 0.257 and glycinate is allowed to react with equimolar of MA, the 18% decrease in the integration of the vinyl signal would indicate the 70% of $[P_{4444}][Gly]$ reacted with MA. From these results there may be a possibility that the deactivation of vinyl group of acrylate monomer by Michael addition of amino acid anion would be occurred. However, if all the $[P_{4444}][Gly]$ react with MA, about 75% of MA ought to be remained after the reaction under the investigated experimental condition. Therefore, there would be another possibility for the inhibition of gel formation.

Polymerization kinetics

To investigate the polymerization kinetics, the FT-IR spectra during polymerization was monitored in real time by using ReactIRTM 15 (Mettler Toledo International Inc.). In this experiment, DMAAm and $[P_{4444}][Pro]$ were chosen as representative examples of a vinyl monomer and AAIL, respectively. In addition, a comparative experiment was performed by polymerizing DMAAm in $[Emim][BF_4]$ which was chosen as a representative unreactive IL. The experiments were carried out as follows. A 3:7 weight ratio mixture of DMAAm and $[P_{4444}][Pro]$ was homogenized by vigorous mixing. The solution was poured into a test tube attached to the diamond ATR-IR-fiber probe of a ReactIRTM 15 and vigorously agitated by a magnetic stirrer. The tip of the probe was immersed in the solution and the test tube was capped with a silicone rubber stopper. The polymerization was initiated by irradiating the solution with 365 nm UV light. Infrared absorption spectra of the samples were measured under continuous UV irradiation. In these experiments, the C=C stretching, in-plane C-H bending and out-of-plane C-H bending of the vinyl group were monitored at 1648, 1421 and 980 cm^{-1} , respectively.

Figure S1(b) shows the raw IR spectra of pure $[P_{4444}][Pro]$, and processed DMAAm spectra from DMAAm/ $[P_{4444}][Pro]$ and DMAAm/ $[Emim][BF_4]$ mixtures, extracted by deducting the spectra of each ionic liquid from the corresponding raw IR spectra of the mixtures before polymerization. As shown in Figure S1(b), the peaks at 1648, 1421 and 980 cm^{-1} for DMAAm, are indicated by broken black lines, and showed little overlap with the characteristic peaks of $[P_{4444}][Pro]$.

The results of monitoring the IR peak around 980 cm^{-1} are shown in Figure S1(c). For polymerization of DMAAm in $[Emim][BF_4]$, the peak corresponding to the out-of-plane C-H bending at 980 cm^{-1} decreased immediately after polymerization was started. Relatively slow attenuation of the corresponding peak intensity was observed during polymerization of DMAAm in $[P_{4444}][Pro]$. The changes of the peak intensities at 1648, 1421 and 980 cm^{-1} during the course of the

polymerization reaction are shown in Figure S1(d). The vertical axis in Figure S1(d) is the differential absorbance intensity values between at certain periods of reaction and at $t = 180$ min. We confirmed from the ^1H NMR measurement that the polymerization reaction in $[\text{P}_{4444}][\text{Pro}]$ was completely finished at $t = 180$ min; i.e. the vinyl signals (δ 5.5–7.0 ppm) for the mixture of DMAAm and $[\text{P}_{4444}][\text{Pro}]$ were completely disappeared (Figure S1(e)).

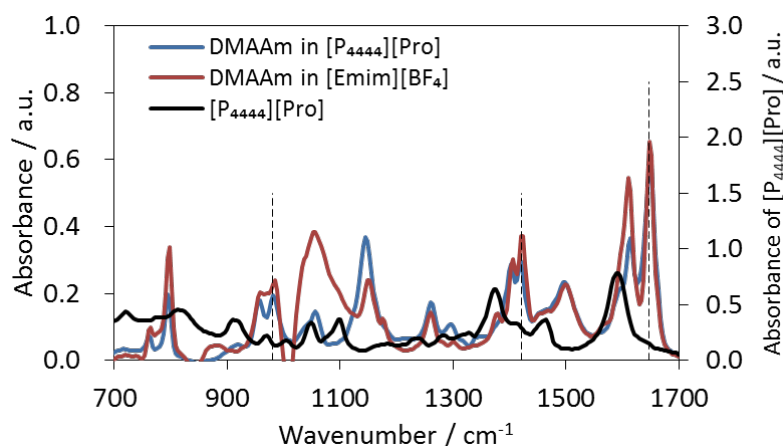


Figure S1(b) IR spectra of $[\text{P}_{4444}][\text{Pro}]$ and the DMAAm spectra in DMAAm/ $[\text{P}_{4444}][\text{Pro}]$ and DMAAm/ $[\text{Emim}][\text{BF}_4]$ mixtures.

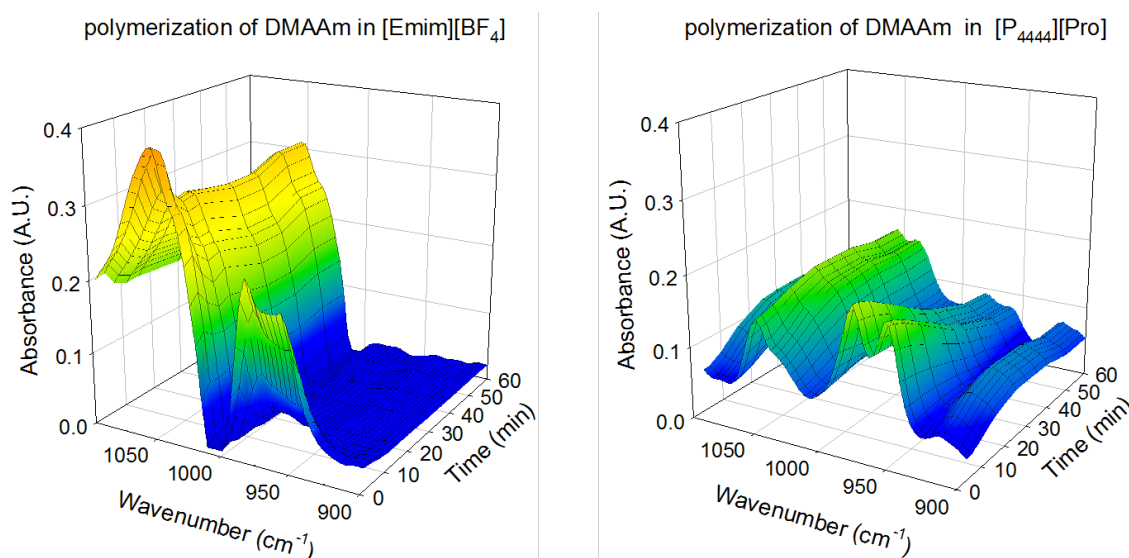


Figure S1(c) Monitored IR peak around 980 cm^{-1} for polymerization of DMAAm in $[\text{Emim}][\text{BF}_4]$ (left) and in $[\text{P}_{4444}][\text{Pro}]$ (right).

As shown in Figure S1(d), similar trends in the absorbance intensity changes at 980 cm^{-1} were also found at 1648 and 1421 cm^{-1} . These results indicated that the propagation rate of DMAAm was reduced in $[\text{P}_{4444}][\text{Pro}]$. From the results shown above, the polymerization rate may be considered to

contribute to the degree of gelation of the AAILs.

Some Research on the propagation and termination kinetics of free radical polymerization in ILs has been reported.³ In these studies, imidazolium-based unreactive ionic liquids were used as the solvent for vinyl monomers and it was shown that the propagation rate increased considerably in the presence of the ILs. As shown in Figure S1(d), it was confirmed that the polymerization rate of DMAAm in [Emim][BF₄] is rapid, in agreement with previous reports. However, for the polymerization of DMAAm in [P₄₄₄₄][Pro], the polymerization rate decreased drastically, in contrast to the previously reported trend. Solvent properties and interactions such as the polarity, electron pair acceptor-electron pair donator interactions and nonspecific (Coulomb) interactions may contribute to the enhancement of the rate of the free radical polymerization of a vinyl monomer. For the AAILs, hydrogen bonding interactions might also contribute because AAILs show strong hydrogen bonding.

Regarding the traditional free radical bulk polymerization, Lee *et al.* reported that more electron-deficient acrylate double bonds undergo faster radical addition reactions than electron-rich double bonds.⁴ This is also unlike the radical polymerization in AAILs shown in this work; i.e., the monomer with large *e*-value cannot gel AAILs and vice versa.

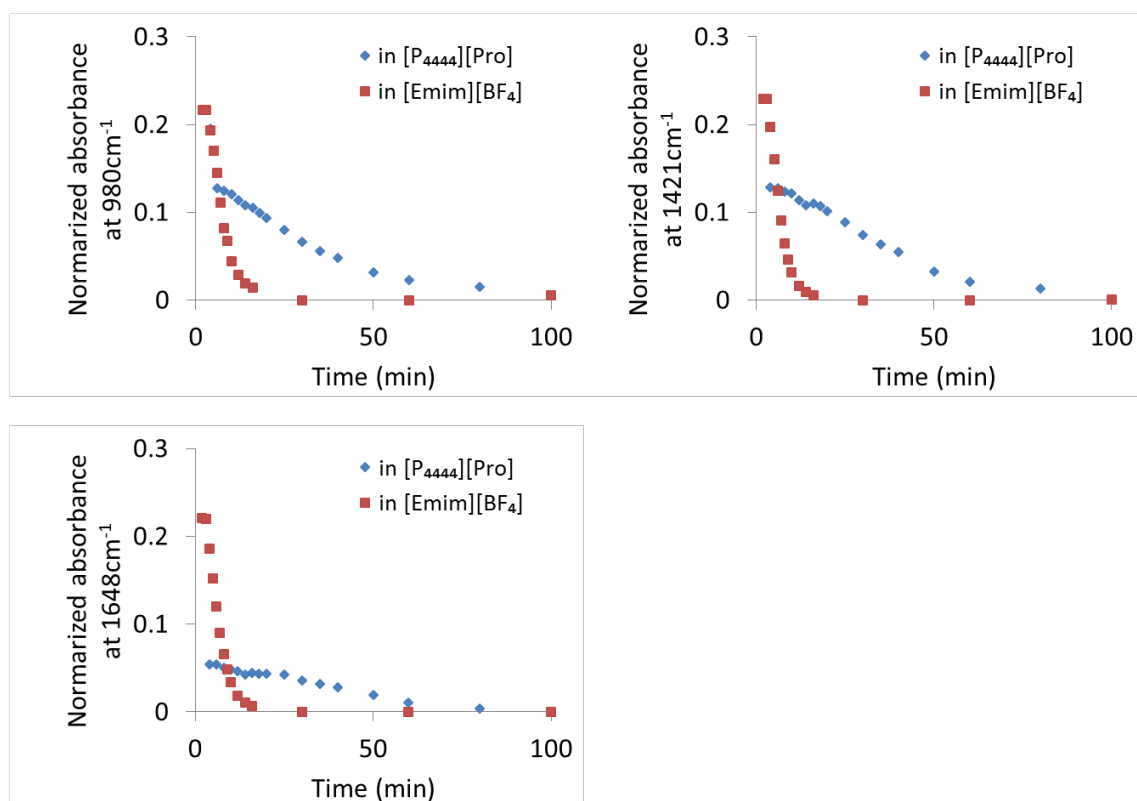


Figure S1(d) Change of the absorbance intensity at 980, 1421 and 1648 cm⁻¹ during polymerization reaction.

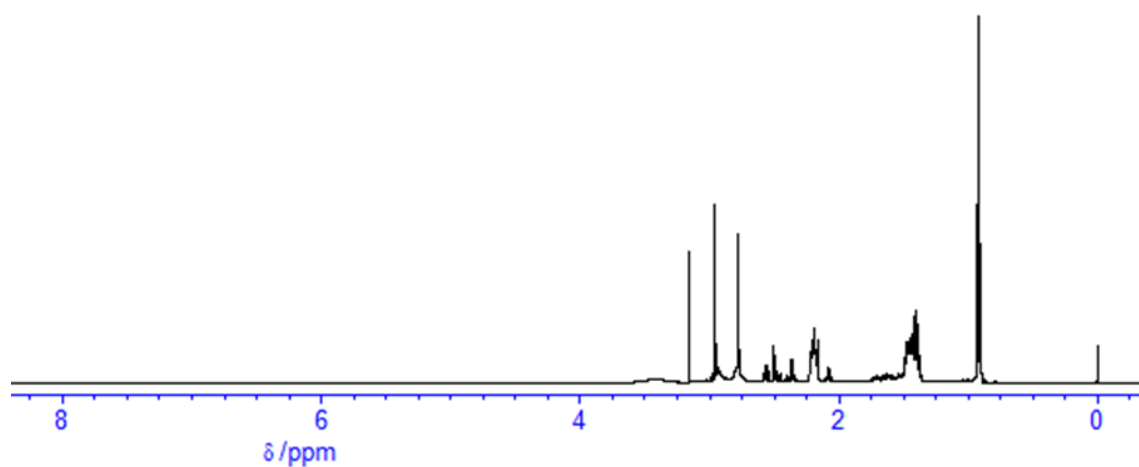


Figure S1(e) ^1H NMR spectrum for DMAAm in $[\text{P}_{444}][\text{Pro}]$ after UV irradiation for 3 h.

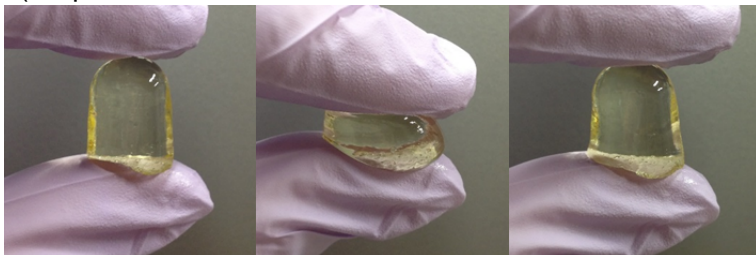
The inhibition of radical polymerization in the presence of AAILs is not well understood at this stage, however further experiments are currently in progress to determine the true cause of the observed inhibition. Understanding the mechanism of inhibition may help us to design controlled polymerization systems to further improve the properties of the AAIL-gels. More detailed investigations of the polymerization kinetics are necessary to understand the inhibition of radical polymerization by AAILs.

(3) Finger-pressure compression tests of AAIL-gels

The results of finger pressure compression tests of $[P_{4444}][Pro]$ -DMAAm gel and $[P_{4444}][Pro]$ -PVP gel are shown in Figs. S2(a) and S2(b). Both the ion-gels maintained their shape before and after compression without any “blow out” of $[P_{4444}][Pro]$ from the polymer matrix.

(a) $[P_{4444}][Pro]$ -PDMAAm gel

(Preparation conditions: DMAAm = 30 wt%, cross-linker/monomer mole fraction = 0.3 (-))



(b) $[P_{4444}][Pro]$ -PVP gel

(Preparation conditions: NVP = 30 wt%, cross-linker/monomer mole fraction = 0.3 (-))

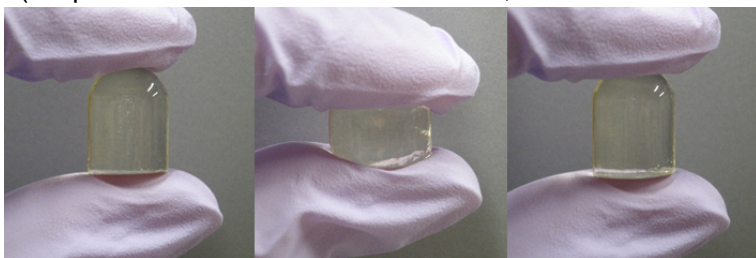


Fig. S2 Photographs of finger pressure compression tests of (a) $[P_{4444}][Pro]$ -DMAAm gel and (b) $[P_{4444}][Pro]$ -PVP gel.

(4) General procedures for AAIL-gel film preparation

A typical procedure for preparation of the AAIL gel films is as follows. Monomer (NVP or DMAAm) and $[P_{4444}][Pro]$ were mixed in a 1:1 weight ratio, and the mixture homogenized by vigorous mixing. EGDMA (molar ratio of EGDMA/monomer = 0.3) was then added, and the mixture homogenized again. Finally, HCPK (weight ratio of HCPK/(monomer+EGDMA) = 0.01) was added and the mixing step repeated a final time. The solution was cast onto a 50 × 50 mm Rain-X-coated quartz substrate. Rain-X is a commercially available, hydrophobic coating for glass surfaces, which aids in the removal of the film after photopolymerization is completed. A 300 μm thick PTFE spacer and identical quartz plate was then placed on top to completely spread the monomer. The plates were placed under a 365 nm UV light for 3 h. After the reaction was complete, the plates were separated and the so formed gel film was peeled-off from the plates. The gel film obtained was flexible and freestanding with a thickness of about 300 μm.

(5) General procedures for gas permeability testing

CO₂ and N₂ gases of 99.9% purity were used for gas permeation tests. A schematic of the experimental apparatus is shown in Fig. S3(a). The gas transport properties of the membrane were measured by using a flat-type permeation cell (Fig. S3(b)) that was placed in a thermostat oven (YAMATO Scientific Co. Ltd., Japan) adjusted to the desired temperature. The permeation cell (GTR TEC Co., Japan) was made of stainless steel with an effective permeation area of 9.51 cm².

A model feed gas was prepared by mixing CO₂ and N₂ without steam. The flow rates of CO₂ and N₂ were controlled by mass flow controllers (Hemmi Slide Rule Co. Ltd., Japan) to adjust the mole fraction of each gas. The total flow rate of the feed gas was adjusted to 1.49×10^{-4} mol/s at 298 K, 101.3 kPa. The flow rates of the feed streams were measured by soap-film flow meters (HORIBA STEC Ltd., Japan). The feed gas was pre-heated by a coiled heat exchanger and introduced into the cell. The permeability tests were carried out at 373 K. The feed side pressure was maintained at atmospheric pressure.

Helium was supplied to the permeate side of the cell as a sweep gas through a coiled heat exchanger at the flow rate of 2.98×10^{-5} mol/s at 298 K, 101.3 kPa. The flow rates of the sweep gas were also measured by soap-film flow meters (HORIBA STEC Ltd.). The pressure on the sweep side was also maintained at almost atmospheric pressure.

The sweep gas containing the permeated CO₂ and N₂ through the AAIL-gel films was sent to a gas chromatograph (Shimadzu GC-8A, column: activated carbon, 1 m) to determine the composition of permeate. An example of time course of permeabilities of CO₂ and N₂ is shown in Fig. S3(c).

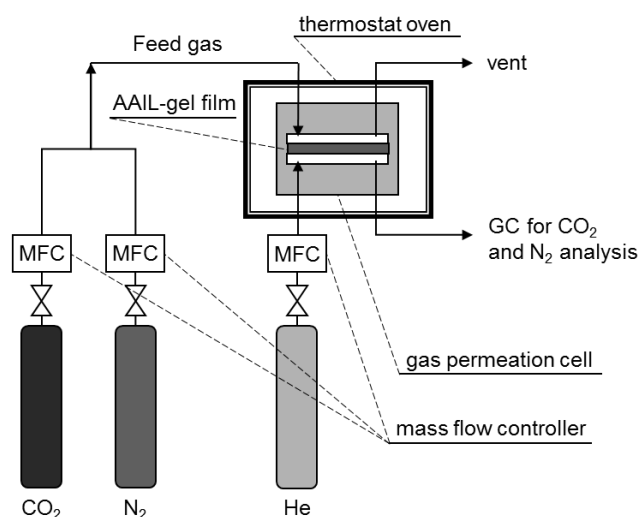


Fig. S3(a) Schematic of the apparatus for gas permeation test

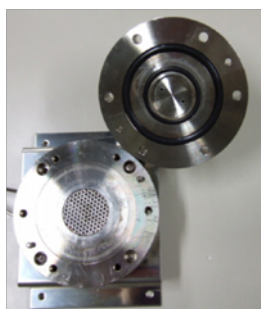


Fig. S3(b) Stainless steel flat-type permeation cell

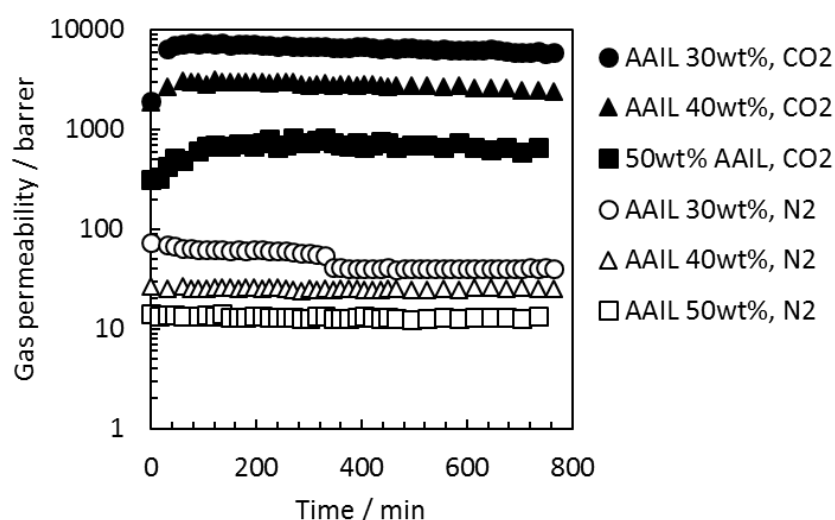


Fig. S3(c) Time course of CO₂ and N₂ permeability through [P₄₄₄₄][Pro]-PVP gel film ($T = 373$ K, Feed mixed gas: CO₂/N₂ (2.5/97.5vol%), Sweep gas: Helium, feed-side and sweep-side pressure were atmospheric pressure, CO₂ partial pressures in feed and sweep gases were 2.5 kPa and 0 kPa, respectively, relative humidity = 0%)

(6) Comparison of the performances of ionic liquid-based CO₂ separation membranes

The permeability and selectivity data for the AAIL-gel films prepared in this work are plotted along with the data for supported ionic liquid membranes (SILMs), ion-gel films (RTIL-gel films), polymeric ionic liquid membranes (poly(RTIL) membranes) and supported AAIL membranes (AAIL-FTMs) in Figure S4(a).^{1,5} In this figure, a well-known “Robeson upper bound” for dense polymer membranes is also shown.⁶ As shown in this figure, most of the performances of the AAIL-gel films are higher than the upper bounds for polymer membranes as well as the performances of SILMs, RTIL-gel films and poly(RTIL) membranes. The superior transport properties of AAIL-gel films stem from the fact that the AAIL in the gel act as a CO₂ carrier. That is to say, the CO₂ permeation mechanism of the AAIL-gel films are facilitated transport mechanism.

This was supported by the relationship between the CO₂ permeability and CO₂ partial pressure. In Figure S4(b), the relationship between the CO₂ permeability of [P₄₄₄₄][Pro]-PVP gel film and CO₂ partial pressure was plotted. It is clearly shown that the CO₂ permeability was decreased with the increase of CO₂ partial pressure. This is well known tendency for facilitated transport membranes (FTMs). The CO₂ permeability of FTMs decreased with the increase of CO₂ partial pressure owing to the carrier saturation with CO₂ under high CO₂ partial pressure conditions. From the another point of view, as shown in Figure S4(a), the CO₂ permeation performance of the AAIL-gel films were very close to those of the AAIL-FTMs. This result also supports the facilitated CO₂ transport mechanism of the AAIL-gel film. A little inferior performance of the AAIL-gel films might be caused by the diffusion resistance due to the PVP matrix in the gel. In fact, the CO₂ permeation performance of the AAIL-gel films approaches those of AAIL-FTMs with the decrease of the polymer ratio in the AAIL-gel. Such trend was also appeared for the membranes containing RTILs. The most SILMs show higher CO₂ permeability than RTIL-gel films which have the better performance than poly(RTIL) membranes. These trend also due to the diffusion resistance caused by the polymer matrix in the membranes.

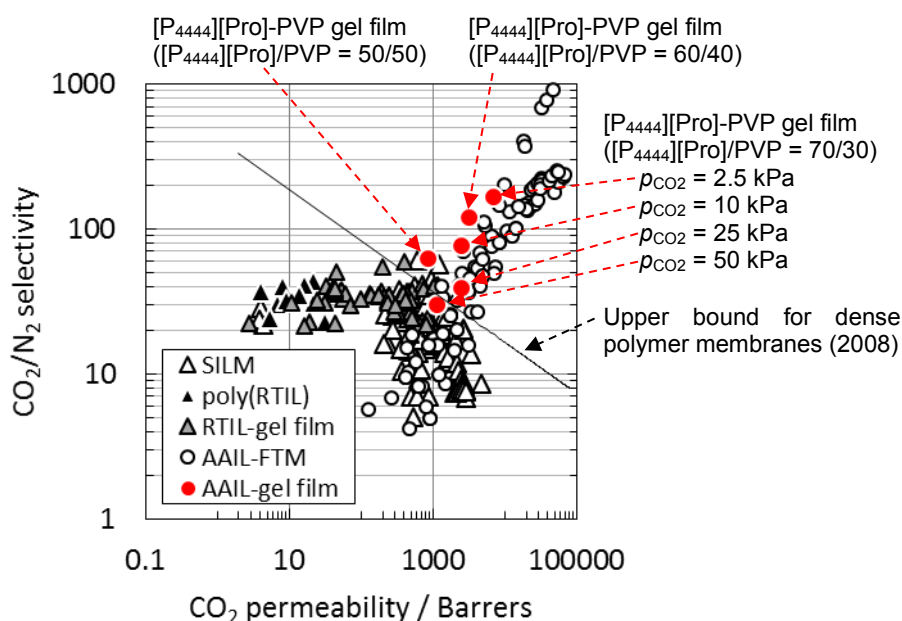


Fig. S4(a) Comparison of gas separation performance for various ionic liquid-related membranes.

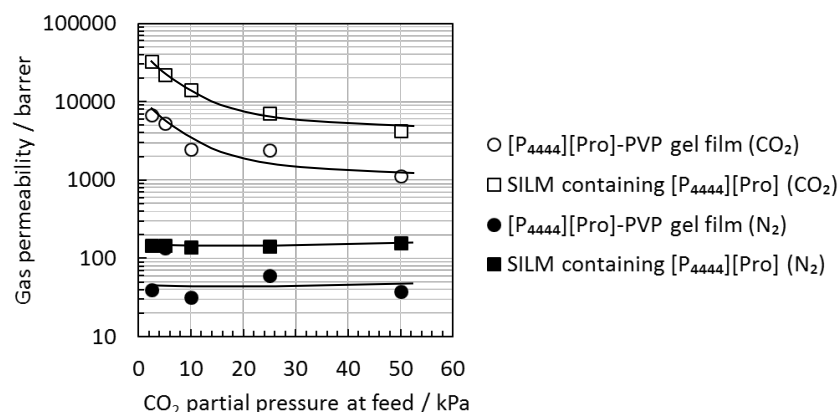


Fig. S4(b) CO₂ partial pressure dependencies on CO₂ permeability of the [P₄₄₄₄][Pro]-PVP gel film of which [P₄₄₄₄][Pro] content was 70wt% ($T = 373$ K, Feed mixed gas: CO₂/N₂ (2.5/97.5, 10/90, 25/75 and 50/50vol%), Sweep gas: Helium, feed-side and sweep-side pressure were atmospheric pressure, CO₂ partial pressures in feed gas were 2.5, 10, 25 and 50 kPa and in sweep gas was 0 kPa, respectively, relative humidity = 0%).

References

1. S. Kasahara, E. Kamio, T. Ishigami and H. Matsuyama, *J. Membr. Sci.*, 2012, **415-416**, 168.
2. (a) D. C. Cole, *Tetrahedron*, 1994, **50**, 9517; (b) E. S. Read, K. L. Thompson and S. P. Armes, *Polym. Chem.*, 2010, **1**, 221.
3. (a) S. Harrisson, S. R. Mackenzie and D. M. Haddleton, *Chem. Commun. (Cambridge, U. K.)*, 2002, 2850; (b) J. Barth, M. Buback, G. Schmidt-Naake and I. Woecht, *Polymer*, 2009, **50**, 5708; (c) A. Jelcic, S. Beuermann and N. Garcia, *Macromolecules (Washington, DC, U. S.)*, 2009, **42**, 5062; (d) I. Woecht, G. Schmidt-Naake, S. Beuermann, M. Buback and N. Garcia, *J. Polym. Sci., Part A: Polym. Chem.*, 2008, **46**, 1460; (e) S. Beuermann, M. Buback, P. Hesse and I. Lacik, *Macromolecules*, 2006, **39**, 184.
4. T. Y. Lee, T. M. Roper, E. S. Jonsson, C. A. Guymon and C. E. Hoyle, *Macromolecules*, 2004, **37**, 3606.
5. (a) S. M. Mahurin, T. Dai, J. S. Yeary, H. Luo and S. Dai, *Ind. Eng. Chem. Res.*, 2011, **50**, 14061; (b) T. K. Carlisle, J. E. Bara, A. L. Lafrate, D. L. Gin and R. D. Noble, *J. Membr. Sci.*, 2010, **359**, 37; (c) Y. C. Hudiono, T. K. Carlisle, J. E. Bara, Y. Zhang, D. L. Gin and R. D. Noble, *J. Membr. Sci.*, 2010, **350**, 117; (d) B. A. Voss, J. E. Bara, D. L. Gin and R. D. Noble, *Chem. Mater.*, 2009, **21**, 3027; (e) J. E. Bara, R. D. Noble and D. L. Gin, *Ind. Eng. Chem. Res.*, 2009, **48**, 4607; (f) J. E. Bara, T. K. Carlisle, C. J. Gabriel, D. Camper, A. Finotello, D. L. Gin and R. D. Noble, *Ind. Eng. Chem. Res.*, 2009, **48**, 2739; (g) J. E. Bara, C. J. Gabriel, T. K. Carlisle, D. E. Camper, A.

- Finotello, D. L. Gin and R. D. Noble, *Chem. Eng. J. (Amsterdam, Neth.)*, 2009, **147**, 43; (h) J. E. Bara, D. L. Gin and R. D. Noble, *Ind. Eng. Chem. Res.*, 2008, **47**, 9919; (i) J. E. Bara, E. S. Hatakeyama, D. L. Gin and R. D. Noble, *Polym. Adv. Technol.*, 2008, **19**, 1415; (j) J. E. Bara, C. J. Gabriel, E. S. Hatakeyama, T. K. Carlisle, S. Lessmann, R. D. Noble and D. L. Gin, *J. Membr. Sci.*, 2008, **321**, 3; (k) J. E. Bara, E. S. Hatakeyama, C. J. Gabriel, X. Zeng, S. Lessmann, D. L. Gin and R. D. Noble, *J. Membr. Sci.*, 2008, **316**, 186; (l) J. E. Bara, S. Lessmann, C. J. Gabriel, E. S. Hatakeyama, R. D. Noble and D. L. Gin, *Ind. Eng. Chem. Res.*, 2007, **46**, 5397; (m) Y.-Y. Gu and T. P. Lodge, *Macromolecules (Washington, DC, U. S.)*, 2011, **44**, 1732; (n) Y. Gu, E. L. Cussler and T. P. Lodge, *J. Membr. Sci.*, 2012, **423-424**, 20; (o) J. C. Jansen, K. Friess, G. Clarizia, J. Schauer and P. Izak, *Macromolecules (Washington, DC, U. S.)*, 2011, **44**, 39; (p) T. K. Carlisle, G. D. Nicodemus, D. L. Gin and R. D. Noble, *J. Membr. Sci.*, 2012, **397-398**, 24; (q) P. Scovazzo, *J. Membr. Sci.*, 2009, **343**, 199; (r) J. J. Close, K. Farmer, S. S. Moganty and R. E. Baltus, *J. Membr. Sci.*, 2012, **390-391**, 201; (s) S. U. Hong, D. Park, Y. Ko and I. Baek, *Chem. Commun. (Cambridge, U. K.)*, 2009, 7227; (t) S. Kasahara, E. Kamio, T. Ishigami and H. Matsuyama, *Chem. Commun. (Cambridge, U. K.)*, 2012, **48**, 6903; (u) L. C. Tome, M. A. Aboudzadeh, L. P. N. Rebelo, C. S. R. Freire, D. Mecerreyes and I. M. Marrucho, *J. Mater. Chem. A*, 2013, **1**, 10403; (v) P. Scovazzo, J. Kieft, D. A. Finan, C. Koval, D. DuBois and R. Noble, *J. Membr. Sci.*, 2004, **238**, 57.
6. L. M. Robeson, *J. Membr. Sci.*, 2008, **320**, 390.